THE JOURNAL OF BIOLOGICAL CHEMISTRY
Vol. 274, No. 36, Issue of September 3, pp. 25945–25952, 1999

Printed in U.S.A.

Amyloid β-Protein Fibrillogenesis

STRUCTURE AND BIOLOGICAL ACTIVITY OF PROTOFIBRILLAR INTERMEDIATES*

(Received for publication, March 31, 1999, and in revised form, June 18, 1999)

Dominic M. Walsh‡, Dean M. Hartley‡, Yoko Kusumoto§, Youcef Fezoui‡, Margaret M. Condron‡, Aleksey Lomakin‡§, George B. Benedek§, Dennis J. Selkoe‡, and David B. Teplow‡¶

From the ‡Center for Neurologic Diseases, Brigham & Women's Hospital and Harvard Medical School, Boston, Massachusetts 02115 and the §Department of Physics and Center for Material Science and Engineering, Massachusetts Institute of Technology, Cambridge, Massachusetts 02139

Alzheimer's disease is characterized by extensive cerebral amyloid deposition. Amyloid deposits associated with damaged neuropil and blood vessels contain abundant fibrils formed by the amyloid β-protein (Aβ). Fibrils, both *in vitro* and *in vivo*, are neurotoxic. For this reason, substantial effort has been expended to develop therapeutic approaches to control Aβ production and amyloidogenesis. Achievement of the latter goal is facilitated by a rigorous mechanistic understanding of the fibrillogenesis process. Recently, we discovered a novel intermediate in the pathway of Aβ fibril formation, the amyloid protofibril (Walsh, D. M., Lomakin, A., Benedek, G. B., Condron, M. M., and Teplow, D. B. (1997) *J. Biol. Chem.* 272, 22364–22372). We report here results of studies of the assembly, structure, and biological activity of these polymers. We find that protofibrils: 1) are in equilibrium with low molecular weight Aβ (monomeric or dimeric); 2) have a secondary structure characteristic of amyloid fibrils; 3) appear as beaded chains in rotary shadowed preparations examined electron microscopically; 4) give rise to mature amyloid-like fibrils; and 5) affect the normal metabolism of cultured neurons. The implications of these results for the development of therapies for Alzheimer's disease and for our understanding of fibril assembly are discussed.

Alzheimer's disease (AD)[1] is a progressive neurodegenerative disorder defined histologically by the formation in the brain of intracellular neurofibrillary tangles and extracellular amyloid deposits (1). Particular attention has been focused on the role that the amyloid β-protein (Aβ), the primary protein constituent of amyloid deposits, plays in development of AD. Aβ molecules are fibrillogenic and exist in a number of forms *in vivo* (2). Among those forms found in amyloid deposits, 40 and 42 residue long species (Aβ(1–40) and Aβ(1–42), respectively) are particularly important. Genetic studies of AD have shown that mutations in the gene encoding the precursor of Aβ (the amyloid β-protein precursor (βAPP) gene) (3–6), or in genes that regulate the proteolytic processing of βAPP (7–9), cause AD. The phenotypic effects of these mutations show remarkable consistency, they all result in excessive production of Aβ or in an increased Aβ(1–42)/Aβ(1–40) ratio, facilitating amyloid deposition (10, 11). In addition, specific haplotypes and mutations in genes involved in the extracellular transport or cleavage of Aβ are risk factors for AD (12, 13). *In vitro* and *in vivo* studies of Aβ toxicity indicate that fibrillar Aβ can directly kill neurons or initiate a cascade of events leading to neuronal cell death (14–16). For this reason, therapeutic strategies targeting Aβ fibrillogenesis are being pursued actively (17–20). Unfortunately, key areas of Aβ fibrillogenesis are poorly understood. In particular, the three-dimensional structure and organization of fibril subunits are unknown, as are the steps involved in assembly of nascent, monomeric Aβ first into nuclei, then into higher order oligomers and polymers. Identification of structural intermediates in the fibrillogenesis process and elucidation of the thermodynamics of the associated conformational changes in, and assembly of, Aβ will facilitate identification of therapeutic targets.

Rigorous biophysical studies of fibrillogenesis require well characterized, homogeneous starting peptide preparations, free of pre-existing fibrillar material, particulates, or other types of fibril seeds. In prior studies, synthetic Aβ has been dissolved in water or in organic solvents, then diluted directly into buffer for use (21–24). It has been demonstrated that when synthetic Aβ peptides are resuspended at neutral pH they contain a heterogeneous mixture of different sized species (25, 26). In some cases, attempts to physically "de-seed" stock peptide solutions have been made (21). However, in most studies, either no precautions were taken or filtration through 0.2-μm filters, incapable of removing anything other than large aggregates, was used. The use of these solutions complicates data interpretation and precludes the study of the earliest phases of fibrillogenesis *in vitro*. We recently demonstrated that size exclusion chromatography (SEC) can be used to prepare homogeneous populations of Aβ, termed low molecular weight Aβ (LMW Aβ), which are composed of monomeric or dimeric Aβ molecules (26). Using these preparations to study Aβ fibrillogenesis, we discovered and reported the initial characterization of a new fibrillogenesis intermediate, the amyloid protofibril (26). This intermediate was also described independently by Harper *et al.* (22). Protofibrils are short, flexible fibrils, generally 4–10 nm in diameter and up to 200 nm in length, as measured by negative staining and electron microscopy. Protofibrils appear transiently during Aβ fibrillogenesis (26, 27). Evidence suggests that protofibrils are precursors of the longer,

* This work was supported by National Institutes of Health Grants 1P01 AG14366 (to D. B. T.), 1R01 NS38328 (to D. B. T.), and 1R01 AG12749 (to D. J. S.), through the generosity of the Foundation for Neurologic Diseases, and Amgen/MIT and Amgen/Brigham and Women's Hospital research collaboration agreements. The costs of publication of this article were defrayed in part by the payment of page charges. This article must therefore be hereby marked "*advertisement*" in accordance with 18 U.S.C. Section 1734 solely to indicate this fact.

¶ To whom correspondence should be addressed: Center for Neurologic Diseases, Brigham & Women's Hospital, 77 Ave. Louis Pasteur (HIM756), Boston, MA 02115. Tel.: 617-525-5270; Fax: 617-525-5252; E-mail: teplow@cnd.bwh.harvard.edu.

[1] The abbreviations used are: AD, Alzheimer's disease; Aβ, amyloid β-protein; βAPP, amyloid β-protein precursor; SEC, size exclusion chromatography; LMW, low molecular weight; AAA, amino acid analysis; QLS, quasielastic light scattering spectroscopy; ThT, thioflavin T; MTT, 3-(4,5-dimethylthiazol-2-yl)-2,5-diphenyltetrazolium bromide; AFM, atomic force microscopy.

more rigid, amyloid-type fibrils typically produced *in vitro* using synthetic peptides (22, 26). If an analogous fibril maturation mechanism operates *in vivo*, the protofibril stage could be an important therapeutic focus. This may, in fact, be the case as soluble oligomeric forms of Aβ have been isolated from human AD brain (28). We report here results of studies which significantly extend our knowledge of protofibril morphology, the kinetics and equilibria of protofibril formation and disappearance, the secondary structure of protofibrils and their LMW Aβ precursors, and the biological activity of protofibrils. Our findings suggest that in developing therapies targeting Aβ toxicity, consideration must be given not only to the effects of mature, amyloid-type fibrils, but also to those of protofibrils, and potentially, protofibril precursors.

EXPERIMENTAL PROCEDURES

Chemicals and Reagents—Chemicals were obtained from Sigma and were of the highest purity available. Water was double-distilled and deionized using a Milli-Q system (Millipore Corp., Bedford, MA). Tissue culture components were obtained from Life Technologies, Inc. (Grand Island, NY).

Peptides—Aβ(1–40) was synthesized and purified in our laboratory as described (26). Peptide mass, purity, and quantity were determined by a combination of matrix-assisted laser desorption/ionization time-of-flight mass spectrometry, analytical high performance liquid chromatography, and quantitative amino acid analysis (AAA). Purified peptides were aliquoted, lyophilized, and stored at −20 °C until used. Aβ(1–40) was also obtained from Bachem (Torrance, CA) and Quality Controlled Biochemicals (Hopkington, MA). Estimates of peptide content were provided by each manufacturer. Iodinated Aβ(1–40) (^{125}I-Aβ(1–40); ~2000 Ci/mmol in 35% (v/v) acetonitrile, 0.1% (v/v) trifluoroacetic acid) was generously provided by Dr. Evelyn R. Stimson, University of Cincinnati College of Medicine.

Size Exclusion Chromatography (SEC) System—A Superdex 75 HR 10/30 column (Amersham Pharmacia Biotech, Piscataway, NJ) was attached either to a Waters 650 Advanced Protein Purification system, consisting of a Waters 650 controller and pump, a Rheodyne 9125 injector, a Waters 484 tunable absorbance detector, and a Waters 745 data module, or to a Beckman 110B solvent delivery system module 406 and System Gold detector module 166.

Isolation of Low Molecular Weight Aβ (LMW Aβ)—In this work, the term "low molecular weight Aβ" (LMW Aβ) signifies an Aβ species which elutes from a SEC column as a single peak and has a hydrodynamic radius consistent with that of either an extended monomer or a compact dimer (determined by quasielastic light scattering spectroscopy (QLS) to be 1–2 nm) (26). To isolate LMW Aβ, Aβ(1–40) was dissolved at a concentration of 2 mg/ml in dimethyl sulfoxide and sonicated in a Branson 1200 ultrasonic water bath for 10 min, after which 200 μl of this solution were injected into the SEC column. The column was eluted with 0.05 M Tris-HCl, pH 7.4, containing 0.02% (w/v) sodium azide, at a flow rate of 0.5 ml/min. Peptides were detected by UV absorbance at 254 nm, and 350-μl volume fractions were collected during elution of the LMW Aβ peak. Pre-dissolution of Aβ in either dimethyl sulfoxide or buffer gave essentially the same results with respect to SEC and subsequent QLS and circular dichroism spectroscopy (CD) analysis, but dimethyl sulfoxide treatment significantly increased the recovery of peptide.

Isolation of Protofibrils—Protofibrils were prepared essentially as described (26). Briefly, 400 μg of Aβ(1–40) were dissolved in 100 μl of water, diluted with an equal volume of 0.2 M Tris-HCl, pH 7.4, containing 0.04% (w/v) sodium azide, then incubated at room temperature for 40–60 h. The yield of protofibrils varied among different peptide lots, but a 1–2-day incubation period generally yielded equivalent amounts of protofibrils and LMW Aβ. Following incubation, the solution was centrifuged at 16,000 × *g* (measured at tube bottom) for 5 min, then ~160 μl of the supernate were fractionated by SEC, as described above. This procedure yields a symmetric peak in the void volume of the column (M_r > 30,000 for dextrans) which contained protofibrils and a peak of LMW Aβ in the included volume (26). Electron microscopic examination of the assemblies in the void peak have revealed small globular structures ~5 nm in diameter and rods with lengths up to ~200 nm. Based on a 4–5-nm diameter rod and a linear density of Aβ molecules of 0.8 nm^{-1} (29), the molecular masses of these assemblies would range from ~25 to 900 kDa.

Electron Microscopy—Samples were prepared for electron microscopy (EM) using both negative contrast and rotary shadowing techniques. Preparation of samples for negative contrast was performed as described (26). Briefly, sample was applied to a carbon-coated Formvar grid, fixed with a solution of glutaraldehyde, then stained with uranyl acetate. Samples were observed using a JEOL 1200 EX transmission electron microscope. For rotary shadowing, casts of samples were prepared essentially as described (30). 100-μl aliquots of protofibril fractions were first diluted in 5 mM imidazole, 50 mM NaCl, to ~1 ml and then diluted with 2 volumes of freshly distilled glycerol. The resulting solution was sprayed onto newly cleaved mica sheets and rotary shadowed using a Denton vacuum evaporator and a platinum source such that an ~1 nm thick sheet of platinum was deposited on the mica. Following this treatment, a thin carbon film was deposited on top of the platinum. The replica was floated off on water and picked up with a 400-mesh copper grid and examined using a JEOL 100 CX transmission electron microscope.

Dialysis of Radiolabeled LMW Aβ and Protofibrils—400 μg of Aβ(1–40) were dissolved in 20 μl of dimethyl sulfoxide, to which was added 10 μl of ^{125}I-Aβ(1–40). This mixture was then diluted with 70 μl of water, 100 μl of 0.2 M Tris-HCl, pH 7.4, containing 0.04% (w/v) sodium azide, and then incubated at room temperature for 48–60 h. Following incubation, the solution was centrifuged at 16,000 × *g* for 5 min and 160 μl of supernate fractionated by SEC, as described above. 200-μl aliquots of the LMW Aβ and protofibril fractions were placed in 1-ml sterile Spectra/Por CE DispoDialyzers (Spectrum Scientific, Laguna Hills, CA) and dialyzed with gentle stirring at room temperature *versus* 20 ml of 0.05 M Tris-HCl, pH 7.4, containing 0.02% (w/v) sodium azide. In addition, other aliquots of the SEC fractions were used for negative contrast EM, AAA, and scintillation counting. To ensure that the ^{125}I-Aβ was accurately tracing the cold peptide, all SEC fractions were subjected to scintillation counting and the radiotracer profile compared with the UV chromatogram. Only samples which showed a similar distribution of radiolabel and UV absorbance were used. In order to monitor the release of LMW ^{125}I-Aβ(1–40) from the dialysis bag, 1-ml aliquots of dialysis buffer were removed and counted. The aliquots were returned to the dialysis chamber after counting (normally <5 min after their removal). At the end of the experiment, the bag was removed, counted, and a sample of the contents taken for negative contrast EM.

Monitoring LMW Aβ and Protofibril Size by QLS—QLS was performed as described previously (26). Briefly, measurements were performed at 25 °C using a Langley Ford model 1097 autocorrelator and a Coherent argon ion laser (Model Innova 90-plus) tuned to 514 nm. LMW Aβ and protofibrils were isolated as described above. To avoid interference from dust, QLS tubes were washed in a continual flow of eluent from a Superdex 75 column and LMW Aβ or protofibril material were collected directly into these tubes by displacement (31). The tubes were then heat-sealed and QLS monitoring begun, usually within 2–5 min of collection.

Preparation of Fibril Standards for Dye-binding Experiments—Fibrils were prepared by dissolving 800 μg of Aβ(1–40) in 200 μl of water and then diluting with an equal volume of 0.2 M Tris-HCl, pH 7.4, containing 0.04% (w/v) sodium azide. This solution was incubated for 5 days at 37 °C, then thoroughly mixed, diluted with an equal volume of water, and an aliquot examined by EM to confirm the presence of mature fibrils. The remaining solution was serially diluted to yield concentrations of approximately 500, 250, 125, 62, 31, and 16 μg/ml in 0.05 M Tris-HCl, pH 7.4. Standards were used immediately or stored at −20 °C until required. The concentrations of the standards were determined by AAA.

Congo Red Binding Assay—Congo red binding was assessed essentially as described by Klunk *et al.* (32), but with volumes adjusted to perform the assay in a microtiter plate. Briefly, 225 μl of 20 μM Congo red in 20 mM potassium phosphate, pH 7.4, containing 0.15 M sodium chloride, was added to 25 μl of sample, mixed, and incubated for 30 min at room temperature. The absorbance of the resulting solutions was then measured at 480 and 540 nm using a Molecular Devices Thermo Max microplate reader. All samples were assessed in triplicate and the amount of Congo red bound (Cb) calculated using the formula Cb (nM) = $[(A_{540}/25{,}295) - (A_{480}/46{,}306)] \times 10^3$. The Cb values shown were obtained after subtraction of Cb values for buffer alone.

Thioflavin T Binding Assay—Thioflavin T (ThT) binding was assessed as described by Naiki and Nakakuki (33). 100 μl of sample was added to a 1-cm path length cuvette containing 800 μl of water and 1 ml of 100 mM glycine-NaOH, pH 8.5. The reaction was then initiated by the addition of 50 μl of 100 μM ThT in water and the solution vortexed briefly. Fluorescence was measured after 90, 100, 110, and 120 s. Measurements were made using a Perkin-Elmer LS-5B Luminescence spectrometer with excitation and emission wavelengths of 446 nm (slit

width = 5 nm) and 490 nm (slit width = 10 nm), respectively. Each sample and standard was done in triplicate.

Circular Dichroism Spectroscopy—Solutions of protofibrils or LMW Aβ isolated by SEC were placed into 1-mm path length quartz cuvettes (Hellma, Forest Hills, NY) and spectra obtained from ~195–250 nm at room temperature using an Aviv 62A DS spectropolarimeter. Raw data were manipulated by smoothing and subtraction of buffer spectra, according to the manufacturer's instructions. Deconvolution of the resulting spectra was achieved using the program CDANAL (34) and the Brahms and Brahms reference library (35). The relative amounts of random coil, α-helix, β-sheet, and β-turn in each sample were determined from the normalized contribution of each secondary structure element function to the observed spectrum following curve fitting.

Preparation of LMW Aβ, Protofibrils, and Fibrils for Biological Activity Studies—LMW Aβ and protofibrils were prepared by SEC. Briefly, 1 mg of peptide was dissolved in 250 μl of water containing 0.01% (v/v) phenol red, diluted with an equal volume of 0.2 M Tris-HCl, pH 7.4, then incubated at room temperature for 2 days. Solutions were then centrifuged at 16,000 × *g* for 5 min and 400–440 μl of the supernate fractionated on a Superdex 75 column eluted with 5 mM Tris-HCl, pH 7.4, 70 mM NaCl, at 0.5 ml/min. The elution solvent was chosen empirically after preliminary experiments showed that 0.05 M Tris buffer was toxic to cultured neurons and that LMW Aβ and protofibril yields were unacceptably low in the absence of salt. The Tris/NaCl system produced chromatograms indistinguishable from those seen using 0.05 M Tris-HCl, pH 7.4. In addition, the morphology and hydrodynamic radii of protofibrils prepared by this method were essentially the same as those obtained using 0.05 M Tris buffer. Peptides were detected by UV absorbance at 254 nm and 450-μl fractions were collected during elution of the LMW Aβ and protofibril peaks. Fractions used for studies of biological activity were also subjected to AAA and EM.

In attempting to produce fibrils, we found that when Aβ(1–40) (from a variety of sources) was dissolved at >1 mg/ml in water, it produced a solution whose pH (<3) could not be adjusted properly with 5 mM Tris buffer. To overcome this problem and facilitate monitoring of the pH under sterile conditions, peptide was suspended initially at ~3.2 mg/ml in 1 mM NaOH, containing 0.01% (v/v) phenol red. 10 mM NaOH then was added at the empirically determined ratio of 200 μl/mg of peptide. This ratio varied slightly among different peptide lots. Finally, the solution was diluted sequentially with 100 mM Tris-HCl, pH 7.4, containing 1.4 M NaCl, and water to give a concentration of ~1.6 mg/ml Aβ(1–40) in 5 mM Tris-HCl, pH 7.4, containing 70 mM NaCl. These solutions were incubated for 2 days at 37 °C, and then used. This procedure consistently produced solutions of amyloid fibrils which could be sedimented readily by brief centrifugation (16,000 × *g*, 5 min) and which were indistinguishable from those formed by incubation in 50 mM Tris-HCl, pH 7.4.

Neuronal Cell Cultures—Rat primary cortical neurons were prepared according to Hartley *et al.* (36), with slight modifications. Briefly, brain cells were isolated from the neocortex of E15-17 rat embryos and plated onto poly-L-lysine coated 96-well plates at a density of 2×10^4 cells/well in Dulbecco's minimal essential medium containing 5% (v/v) bovine calf serum, 10% (v/v) Ham's F-12, HEPES (20 mM), L-glutamine (2 mM), and penicillin-streptomycin (500 units/ml and 500 μg/ml, respectively). Cultures were used 2–4 days after plating.

MTT Assay—Cell-mediated reduction of 3-(4,5-dimethylthiazol-2-yl)-2,5-diphenyltetrazolium bromide (MTT) was assessed according to the method of Hansen *et al.* (37). Freshly isolated protofibrils or LMW Aβ fractions were mixed with concentrated stock solutions of individual tissue culture components to produce a final solution containing 10 mM glucose, 500 units/ml penicillin, 500 μg/ml streptomycin, 20 mM HEPES, and 26 mM $NaCO_3$, all in 1 × minimal essential medium. Peptide concentrations were determined prior to this supplementation. Fibril standards were prepared in a similar fashion to yield nominal final peptide concentrations of 5, 10, and 15 μM. Cells were incubated either in 50 μl of medium without Aβ or in 50 μl containing fibrillar Aβ, protofibrils, or LMW Aβ. After 2 h, 10 μl of 2.5 mg/ml MTT was added to each well and the incubation continued for a further 3 h. Cells were then solubilized in 200 μl of 20% (w/v) SDS in 50% (v/v) *N,N′*-dimethylformamide, 25 mM HCl, 2% (v/v) glacial acetic acid, pH 4.7, by overnight incubation at 37 °C. Levels of reduced MTT were determined by measuring the difference in absorbance at 595 and 650 nm using a Molecular Devices Thermo Max microplate reader. The effects of treatments were compared with controls by using the one-way analysis of variance Tukey test. No reduction of MTT was observed in fibril controls (even at a concentration of ~30 μM) in the absence of cells.

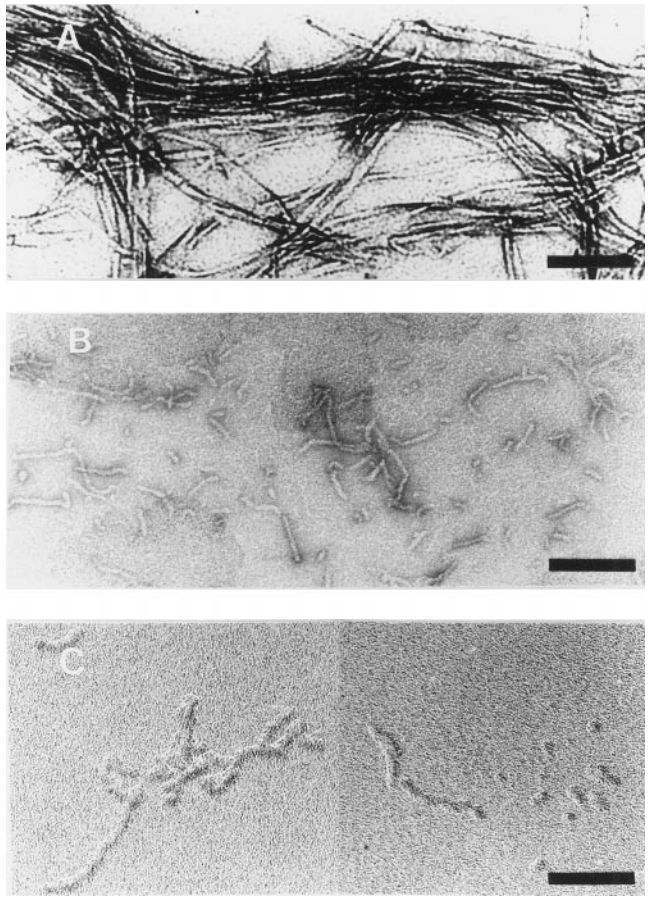

FIG. 1. **Morphology of Aβ fibrils and protofibrils.** Fibrils and protofibrils were prepared from Aβ(1–40) and examined by transmission EM. *A,* negatively stained fibrils; *B,* negatively stained protofibrils; and *C,* rotatory shadowed protofibrils. Plate C is a composite of two regions of the same grid. *Scale bars* are 100 nm. See text for methods.

RESULTS

Morphological Characterization of Protofibrils—Previous studies of protofibril morphology utilizing negative staining and EM (26), or AFM (22, 27), required avid macromolecule adherence to the sample support for their success. If certain structures were washed away during preparation of the supports, potentially important species would not be observed. To address this issue, and to further our efforts at understanding the gross morphology of protofibrils, we performed electron microscopic examination of protofibrils prepared by rotatory shadowing. In this procedure, which involves no washing, a thin, uniform film of sample is sprayed onto a mica support from which shadow casts are then generated and examined. Both shadowed and negatively stained protofibrils appeared as flexible rods of length up to ~200 nm (Fig. 1, *B* and *C*). However, three significant differences were observed between the two preparations. First, the estimated diameters of the shadowed fibrils were larger (8–14 nm compared with 4–7 nm). This was expected due to the accretion of platinum and carbon on the fibrils. Second, the protofibrils appeared more beaded when visualized by rotatory shadowing. The periodicity of this "beading" was 3–6 nm. Third, the proportion of small protofibrils (<10 nm) was higher, suggesting that many of these structures are lost during routine negative staining. The smallest assemblies appear as somewhat imperfect spheres, approximately one fibril diameter in size.

Protofibrils Are in Equilibrium with LMW Aβ—As a first step toward elucidating the structural and kinetic relationships among LMW Aβ and its assemblies, we asked whether

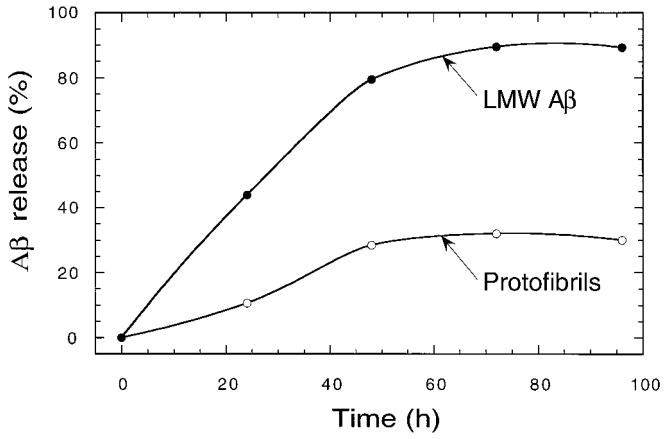

FIG. 2. **Protofibrils are in equilibrium with LMW Aβ.** Radiolabeled protofibrils and LMW Aβ were isolated by SEC and placed in separate dialysis bags (8,000 molecular weight cutoff) which were then incubated at room temperature in separate reservoirs. Periodically, samples from the reservoirs were counted to determine the amount of radiolabeled Aβ diffusing out of the bags. The results shown were typical of the total of seven performed. The starting concentrations of protofibrils and LMW Aβ, as determined by AAA, were 19.2 and 15.5 μM, respectively. Results are expressed as a percentage of the total number of counts originally placed in each bag. Continuous functions were produced by simple smoothing of the line segments joining the data points using the smoothing algorithm resident in the graphing program Kaleidagraph (version 3.0.8).

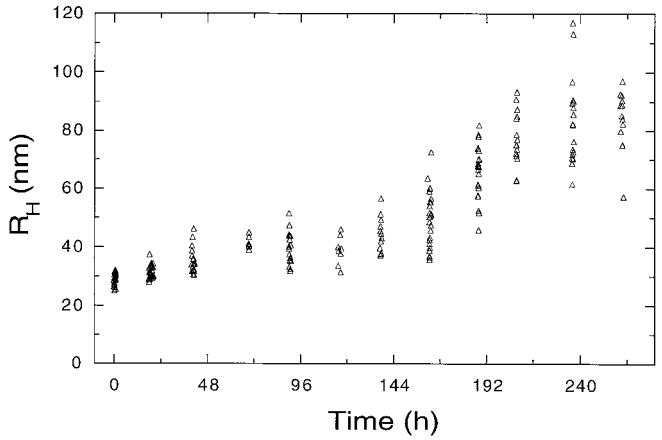

FIG. 3. **Temporal change in protofibril size monitored by QLS.** Protofibrils were isolated by SEC and their average hydrodynamic radii (R_H) were periodically determined using QLS during an 11-day incubation at room temperature. At each monitoring time, multiple determinations were made, each of which is presented in the figure. The total Aβ concentration in the experiment shown was 17 μM.

protofibril formation was an irreversible process or whether an equilibrium existed between protofibrils and LMW Aβ. To do so, radiolabeled protofibrils were isolated by SEC, immediately placed in dialysis bags of 8000 molecular weight cut off, then aliquots of the reservoir removed periodically for counting. Dialysis bags of 8,000 molecular weigh cut off retain >90% of a test solute of molecular weight 8,000 after a 17-h dialysis period. Aβ monomers thus are not retained. The dialysis rate for Aβ dimers is unknown, but would depend on the shape and hydrated volume of these molecules. However, based simply on dimer molecular weight (8,662), release would likely be limited. Representative results from a series of seven experiments are illustrated in Fig. 2. Diffusion of LMW Aβ into the dialysis reservoir was rapid and reproducible, with ~90% of the total counts passing out of the sac within 72 h. The exponential curve shape reflects a simple dialysis process in which free diffusion of solute through the dialysis membrane occurs. Aβ release was also observed from protofibrils, however, it was significantly lower and more variable, with between 18 and 41% of the total counts found in the reservoir after 96 h. In addition, the sigmoidal shape of the release function is consistent with a process in which Aβ must first dissociate from protofibrils before diffusing through the dialysis membrane. The plateauing of the curve at a low level of Aβ release shows that a significant portion of the Aβ present in the dialysis bag is unable to diffuse out. Interestingly, in three of seven experiments, electron microscopic studies revealed typical fibrils (as in Fig. 1*A*) in the dialysis bags after 96 h (data not shown). Protofibrils thus appear to be in equilibrium with LMW Aβ and to give rise to fibrils, from which dissociation of Aβ does not readily occur.

Fibril Formation by Protofibrils—The equilibria found to exist among LMW Aβ, protofibrils, and fibrils complicates the analysis of precursor-product relationships. For example, although unlikely, it is formally possible that protofibrils are reservoirs for LMW Aβ, but do not themselves directly evolve into fibrils. To address this issue, populations of protofibrils were isolated by SEC, then their temporal change in size monitored by QLS. Initially, protofibrils had an average hydrodynamic radius R_H = 27.8 ± 1.8 nm (Fig. 3). This value grew steadily with time, reaching a maximal value of 80.6 ± 14.4 nm at 236 h. For rigid rods, this value of R_H would correspond to lengths of the magnitude of 1 μm. Later, the scattering intensity decreased, a phenomenon routinely observed as large aggregates sediment and leave the illuminated portion of the cuvette. After 263 h, the sealed tube was opened, the contents gently homogenized by pipetting, and aliquots removed for EM and AAA. EM revealed the presence of both fibrils and protofibrils with morphologies similar to those seen in Fig. 1 (data not shown). The EM findings were consistent with the changes in R_H observed by QLS, supporting the hypothesis that protofibrils are direct precursors of fibrils.

Tinctorial Properties of Protofibrils—One of the distinguishing features of amyloid is its capacity to bind the dyes Congo red and thioflavin T, an activity dependent on the presence of extensive arrays of β-pleated sheets (38, 39). In six independent experiments, protofibrils and LMWAβ were isolated by SEC and their ability to bind Congo red compared with that of fibrils. We have observed that protofibril solutions at Aβ concentrations >20 μM readily form fibrils, thus in order to ensure that any dye binding ascribed to protofibrils was not due to fibrils formed *de novo*, Aβ concentrations were kept below 20 μM. In addition, the protofibrillar nature of each sample was confirmed directly by electron microscopy. We found that LMW Aβ, even at concentrations as high as 70 μM, did not bind Congo red, whereas both fibrils and protofibrils did, even at concentrations as low as 2 μM (Fig. 4A). Protofibrils bound Congo red in a concentration-dependent manner, however, variability in this binding was observed, especially at low concentration (<5 μM). This effect is likely due to dissociation of protofibrils into LMW Aβ (which does not bind the dye), a process whose rate may depend on protofibril length and thus could differ among samples due to stochastic variations in the fibril length distributions. Little variability was displayed by fibrils, which also consistently bound slightly higher amounts of dye than did equivalent amounts of protofibrils.

In four of the six Congo red binding experiments, samples were also examined for their ability to bind thioflavin T. As with Congo red, both protofibrils and fibrils, but not LMWAβ, bound thioflavin T (Fig. 4*B*). Interestingly, in two experiments, protofibrils bound more ThT than did equivalent amounts of fibrils (data not shown), whereas the opposite was true in the other two experiments. Absolute values of dye binding can differ depending on the protofibril or fibril preparation. This

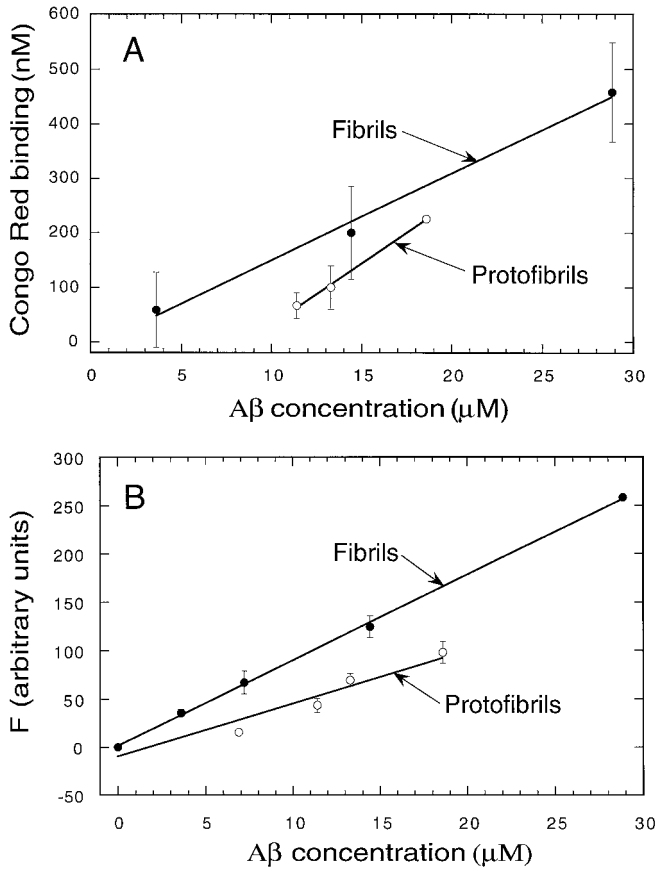

FIG. 4. **Tinctorial properties of fibrils and protofibrils.** Fibrils, protofibrils, and LMW Aβ were treated with Congo red and thioflavin T and the amounts bound determined by absorption or fluorescence, respectively. *A,* Congo red binding was performed in triplicate, on three different samples. Results from a representative experiment are expressed as the average concentration of Congo red bound (nM ± S.D.). In some cases, *error bars* are not obvious because of their small magnitude. Correlation coefficients (r^2) for the concentration dependence lines of fibrils and protofibrils were 0.993 and 0.997, respectively. *B,* thioflavin T binding was measured and plotted in a similar manner. Results are expressed in terms of average fluorescence intensity, *F*, measured in arbitrary units (F ± S.D.). Fibril and protofibril r^2 values were 0.999 and 0.934, respectively.

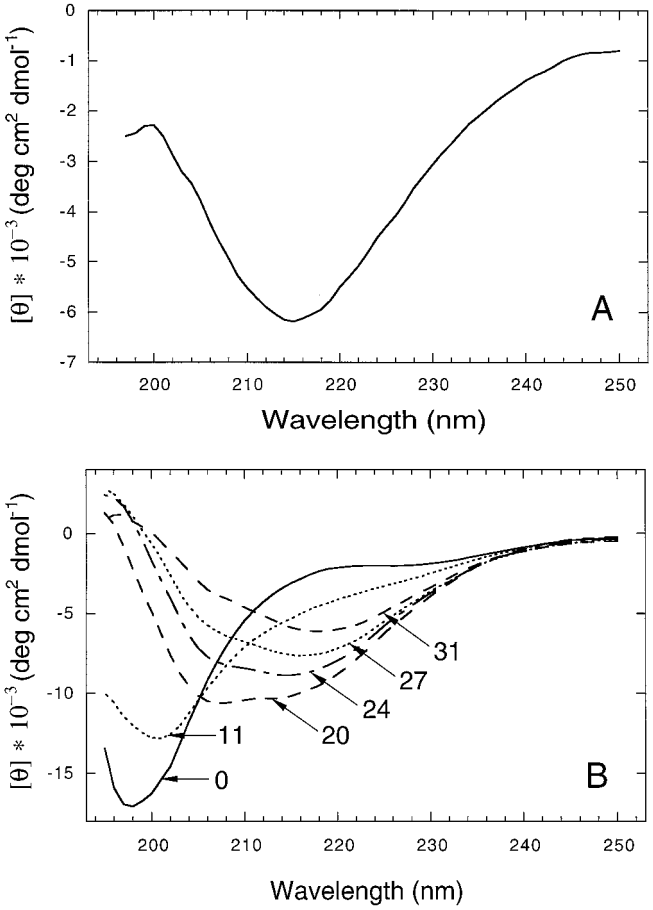

FIG. 5. **Secondary structure analysis of protofibrils and LMW Aβ.** CD spectroscopy was performed on freshly isolated protofibrils (*A*) and LMW Aβ (*B*). Protofibril and LMW Aβ concentrations were 18.5 and 54 μM, respectively. In the case of LMW Aβ, spectra were taken immediately upon isolation, then after 11, 20, 24, 27, and 31 days. Results are expressed as molar ellipticity [Θ] (deg cm^2 dmol^{-1}). The data shown are representative of those obtained in each of five independent experiments.

can occur due to differences in the distribution of polymer sizes, and to post-fibrillogenesis fibril-fibril interactions, which cause equivalent amounts of Aβ to display different binding activities. Nevertheless, the data show clearly that protofibrils bind both Congo red and thioflavin T, a property of amyloid fibrils not possessed by LMW Aβ. This suggests that protofibrils contain significant amounts of β-sheet structure and must thus evolve following significant conformational changes in LMW Aβ.

Secondary Structure of Protofibrils—Numerical estimates of the secondary structure content of protofibrils were obtained using circular dichroism spectroscopy. Protofibrils were isolated by SEC and examined immediately. The prominent features of the resulting spectrum were a minimum at ~215 nm and a maximum at ~200 (Fig. 5*A*). The two low wavelength points of inflection are characteristic of β-sheet structure, however, the negative absolute value of the 200 nm maximum suggests that a significant level of random coil structure exists in the sample. In fact, deconvolution of the spectrum showed 47% β-structure (β-sheet or β-turn), 40% random coil, and 13% α-helix. Examination of numerous other protofibril samples has consistently yielded percentages of β-content ranging from 45 to 50 (data not shown). The β-content of protofibrils is quite similar to that of fibrils (see day 31 data in Table I), even though no fibrils were detected by EM in any of the protofibril samples used for CD. The modest level of α-helix found in protofibrils is interesting in light of the fact that during fibrillogenesis of LMW Aβ, the peptide undergoes a conformational transition from a predominately random coil structure to a β-sheet-rich form, during which a transitory α-helical component is observed (Fig. 5*B* and Table I). In the case of protofibrils, because CD is an averaging technique, it is not possible to say whether the α-helix signal observed emanates from all protofibrils or whether discrete subpopulations of protofibrils or of Aβ monomers or oligomers exist which are significantly richer in this secondary structure element. However, comparative analysis of the CD data from fibrils, protofibrils, and LMW Aβ, does allow the conclusion to be made that protofibrils are a relatively mature stage of the fibrillogenesis process.

Biological Activity of Protofibrils—An important question is whether protofibrils are biologically active. To answer this question, structure-activity studies must be performed rapidly, over a time scale of minutes to hours, before protofibrils produce fibrils. Assays measuring cell death typically require incubation periods of days (40). The MTT assay, in contrast, can reveal physiologic effects induced by treatment of cells with exogenous agents after incubation times of only a few hours (23, 41–43). We thus used this assay to determine whether protofibrils could affect the normal physiology of cultured pri-

TABLE I
Temporal change in Aβ conformation during fibrillogenesis
CD spectra were deconvoluted using the algorithm of Perzcel *et al.* (34) and the Brahms reference spectra library (35). The percentage of each secondary structure element is listed.

Time	Coil	α-Helix	β-Sheet	β-Turn
days				
0	62	11	13	14
11	57	15	17	11
20	46	25	23	6
24	41	20	30	9
27	39	17	31	13
31	37	13	32	18

mary rat cortical neurons. Protofibrils were isolated by SEC and aliquots of the protofibril peak used for the assay, for electron microscopic studies, and for AAA. This procedure ensured that protofibril preparations of proven morphology and known protein concentration were used. We found that protofibrils caused a significant ($p < 0.01$) reduction in the levels of reduced MTT (Fig. 6). As a positive control, preformed Aβ fibrils were also assayed. As expected, fibrils significantly and consistently produced decreases in reduced MTT levels (Fig. 6). Among different experiments, the absolute levels of inhibition caused by protofibrils and fibrils varied, however, in all cases, statistically significant levels of inhibition were observed at Aβ concentrations exceeding ~9 μM. The effect of LMW Aβ was then compared with those of the fibrils and protofibrils. In two experiments, LMW Aβ caused a slight but insignificant increase in levels of reduced MTT (Fig. 6), while in a third experiment, a slight but insignificant decrease was seen (data not shown). These results indicate that protofibrils alter the normal physiology of cultured neurons, whereas LMW Aβ does not.

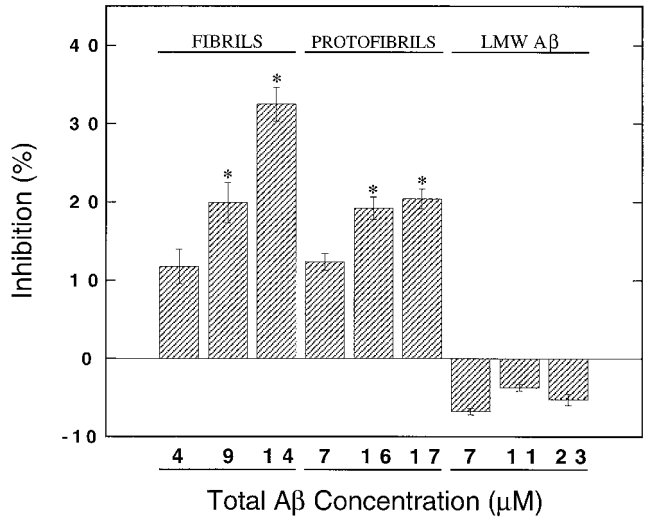

FIG. 6. **Biological activity of protofibrils.** Primary rat cortical neurons were incubated for 2 h with fibrils, protofibrils, LMW Aβ, or medium alone, MTT was added, and then the cells were solubilized 3 h later. Data are expressed as average percent inhibition of MTT reduction ± S.D. ($n \geq 8$), relative to cells treated with medium alone. Total Aβ concentrations (μM) in each treatment group, determined by AAA, are listed on the *abscissa*. The data shown are from a single experiment, but are representative of a total of three independent experiments in which protofibril, fibril, and LMW Aβ concentrations ranged from 6 to 26 μM, 4 to 30 μM, and 6 to 44 μM, respectively. The concentration variation shown for protofibrils was achieved by fractionation of the protofibril peak as it eluted from the SEC column (see "Experimental Procedures"). *Pre facto* preparation of a protofibril dilution series is difficult due to the rapid equilibria among protofibrils, LMW Aβ, and fibrils, which effectively limits protofibril concentration to a maximum of ~20 μM. Relative to medium alone, fibrils and protofibrils both produced significant decreases in levels of reduced MTT (*, $p < 0.01$), while LMW Aβ did not.

DISCUSSION

An intriguing and important area of biomedical research is that of the amyloidoses, a group of diseases caused by the fibrillogenesis and deposition of otherwise soluble and physiologically normal proteins and peptides (38, 39). At least 17 different molecules have been shown to have the capacity, under appropriate conditions, to form amyloid (44). Among these molecules, Aβ is archetypal. Through studies of Aβ fibrillogenesis, therefore, we hope not only to develop therapeutic strategies for Alzheimer's disease, but to elucidate common features of amyloid fibril assembly, thereby accelerating progress toward treatment of other amyloidoses. In the studies reported here, our focus was the assembly, structure, and biological activity of protofibrils, important intermediates in the fibrillogenesis process (22, 26, 27).

In our initial description of protofibrils (26), temporal changes in the levels of LMW Aβ, protofibrils, and fibrils suggested that protofibrils were intermediates in the conversion of LMW Aβ into fibrils. Here, we examined this question directly and found that protofibrils were indeed in equilibrium with LMW Aβ and were capable of forming fibrils. In our dialysis paradigm, the fact that we observed neither complete conversion of protofibrils into fibrils, nor complete protofibril dissociation into LMW Aβ (a range of 18–41% was observed), demonstrates that competing rate constants for protofibril dissociation and fibril formation must be of similar magnitude. The kinetic description of this system is complicated by additional rate constants for protofibril nucleation and elongation. Empirical evidence also suggests that systematic variation in protofibril dissociation rates may occur with protofibril length, further increasing the complexity of this system. Independent of these issues, the most straightforward interpretation of the data is that protofibrils are precursors of fibrils and that fibrils, once formed, do not readily dissociate into protofibrils or LMW Aβ. Irreversible protofibril maturation into fibrils is consistent with the results of our experiments in which temporal increases in average protofibril size were observed by QLS and accompanied by electron microscopically confirmed fibril formation. The same conclusion has been reached in AFM studies of the temporal changes in Aβ polymer structure occurring during fibrillogenesis (22, 27). Our data are also concordant with results of a number of studies showing that Aβ fibrils do not dissociate in the absence of strong chaotropic agents or solvents (28, 45, 46).

Additional support for a protofibril → fibril transition comes from studies designed to elucidate the structural relationships among LMW Aβ, protofibrils, and fibrils. In these experiments, each species was studied using dye binding and CD approaches. Because binding of Congo red and thioflavin T is dependent on the presence of β-sheet structure (47), the data show that protofibrils have significant β-sheet content. Whether statistically significant differences in dye binding exist between protofibrils and fibrils is difficult to determine due to variations in dye binding capacity of different fibril preparations and to the confounding effects of light scattering by different Aβ polymers (48). Interestingly, but not surprisingly, LMW Aβ, even at concentrations up to 70 μM, showed no Congo red or thioflavin T binding, indicating that the assays can differentiate fibrillar and non-fibrillar Aβ. CD data were consistent with the above observations. On average, both protofibrils and fibrils contained substantial and equivalent levels (up to 50%) of β-structure (β-strand and β-turn), along with lesser amounts of random coil (~40%) and α-helix (~10%). LMW Aβ, on the other hand, was predominantly disordered. By these measurements, protofibrils are similar to fibrils and are thus

relatively advanced intermediates in the fibrillogenesis process.

An interesting observation in our study of the temporal change in secondary structure of Aβ during fibril formation was that of a transitory α-helical component. CD and QLS studies showed that LMW Aβ lacked significant ordered structure. However, upon prolonged incubation, a random coil → β-sheet transition was observed, during which the percentage of α-helix rose and fell. Other studies of Aβ(1–40) fibrillogenesis at neutral pH also revealed a random coil → β-sheet transition (49–51). However, to our knowledge, no transitory α-helical component has been described previously under conditions where helix-stabilizing solvents (fluorinated alcohols) were not used. Our ability to observe this transition may result from the use of LMW Aβ rather than Aβ lyophilizates which are simply solvated and used directly. For example, we find that LMW Aβ(1–42) has little regular structure,[2] whereas in other studies of this peptide, even in solutions containing fluorinated alcohols, CD spectra have consistently yielded a high content of β-sheet (49, 52). These contrasting observations suggest that the starting materials used by others contained significant amounts of Aβ aggregates. The significance of the transitory α-helical component is unclear. Because CD is a global averaging method, it is formally possible that not all Aβ molecules conformationally transform through this "α-helix" pathway. However, we feel it is most likely that the conformational transition of Aβ from a predominately unstructured monomer (or dimer) to an assembled β-sheet-rich fibril involves a folding intermediate containing one or more α-helices which then unfold and reform into β-strands. Interestingly, in the case of the scrapie prion protein, a helix → strand folding pathway has, in fact, been postulated to occur during the conversion of the cellular form of the molecule (PrP^{C}) into its scrapie form (PrP^{Sc}) (53, 54). In addition, recent studies of a model 38 residue peptide, αtα (55, 56), have shown that a stable monomeric helical hairpin peptide can rearrange to form classical β-sheet-rich amyloid fibrils.[3]

At the core, both literally and figuratively, formation of amyloid fibrils results from mutually dependent local and global conformational changes in Aβ and its assemblies. We have discussed above certain of the conformational transitions in Aβ occurring during protofibril and fibril formation. We find, as well, that maturation of protofibrils into fibrils may involve subtle alterations in the structural organization of the fibril. In particular, the "beaded" substructure of protofibrils is less prominent in the fibrils. Harper *et al.* (27) have reported a ~20 nm periodic structure in Aβ(1–40) protofibrils studied by AFM. These protofibrils give rise to fibrils in which this period doubles, as does fibril diameter. However, fibrils also form which have diameters approximately equivalent to those of protofibrils and which have a much smoother appearance, a result of substantially less frequent axial discontinuities (often <0.01 nm^{-1}) (27). A granular → smooth transition has been reported by Seilheimer *et al.* (57) during fibril formation by Met(O)-Aβ(1–42). In this study, the authors noted the appearance of large globules and beaded complexes, but these were larger (~30 nm) than those observed here. The protofibril structures observed here may result from the assembly of globular subunits. Small structures of this type have been observed in fibrillogenesis studies of Aβ(1–40) and Aβ(1–42), both using AFM (22, 27, 58) and EM (26, 59). In addition, recent cryoelectron microscopic studies have revealed prominent inhomogeneities within protofibrils, which in some samples appear to derive from the presence of globular subunits.[4] The diameters of the globular assemblies reported here (3–6 nm) are similar to those of ADDLs (58). In fact, this type of small globular assembly may represent a structural unit from which protofibrils are assembled (59). Geometric considerations suggest that as few as 5 or 6 Aβ molecules could constitute this structure. This size is consistent with that of the "β-crystallite" suggested, on the basis of fiber x-ray diffraction studies, to be a building block of Aβ fibrils (60). A pentameric or hexameric building block has also been proposed by the Murphy group (61). It should be noted, however, that depending on the resolution of the visualization method, helices of appropriate pitch can also appear as stacked arrays of globular units.

An important goal in studies of amyloid fibrillogenesis is the correlation of structure with biological activity. In preliminary experiments, treatment of cultured cortical cells with protofibrils or fibrils produced no detectable changes in cell number or LDH release within a time frame (<24 h) precluding maturation of protofibrils into fibrils.[5] We therefore chose to use the MTT assay because it has been shown to be a rapid and sensitive indicator of Aβ-mediated toxicity (23, 41–43). Changes in MTT reduction may reflect alterations in endocytosis, exocytosis, or cellular MTT reductase activity (43, 62, 63). The use of this type of assay, in which effects can be evaluated within 30 min of treatment (43), was critical for allowing a direct correlation between the structures of Aβ assemblies and their biological activities. To measure Aβ-induced cell death requires days of incubation (40), during which protofibrils can be converted to fibrils. This makes determination of the actual active moieties difficult. We found that fibrils and protofibrils both produced highly significant, concentration-dependent decreases in levels of reduced MTT in cultures of rat cortical neurons, whereas no effects were observed for LMW Aβ. Our prior studies of the kinetics of protofibril formation, dissolution, and maturation support the conclusion that the observed effects resulted from the direct interaction of protofibrils, and not fibrils, with the cultured neurons. This conclusion is further corroborated by studies demonstrating that protofibrils (prepared identically to those used here) instantaneously alter the electrical activity of cultured rat cortical neurons (64).[6] Whether the metabolic changes mediated by Aβ are induced at the cell surface by interaction with specific receptors (43, 62) or require internalization of protofibrils or fibrils is currently unknown. However, our results show clearly that whatever the mechanism, protofibrils and fibrils perturb neuronal metabolism whereas LMW Aβ does not. The alteration in neuronal MTT metabolism observed here may be an early indicator of a process leading to neuronal dysfunction and subsequent cell death.

The toxic potential of Aβ has been an area of active investigation since the first demonstration that an Aβ peptide could kill cultured neurons (65). Subsequent studies provided evidence that the Aβ molecule had to be fibrillar to be neurotoxic (66–68), and this observation stimulated the development of strategies to inhibit fibril formation and to dissolve preformed fibrils (17, 18). However, the work reported here, and the recent observation of neurotoxicity of non-fibrillar Aβ-derived diffusible ligands (58), suggest that the notion that only fibrils are toxic must be revisited. For example, if inhibition of fibril formation were to cause an accumulation of protofibrils, Aβ-derived diffusible ligands, or other neurotoxic pre- or non-

[2] D. M. Walsh and D. B. Teplow, unpublished data.

[3] Y. Fezoui and D. B. Teplow, manuscript in preparation.

[4] B. Bohrmann, D. M. Walsh, and D. B. Teplow, unpublished results.

[5] D. M. Walsh, D. M. Hartley, D. J. Selkoe, and D. B. Teplow, unpublished data.

[6] D. M. Hartley, Walsh, D. M., Ye, C. P., Diehl, T. S., Vassilev, P. M., Teplow, D. B., and Selkoe, D. J. submitted for publication.

fibrillar assemblies, this strategy clearly would not be of value. To avoid this outcome, a better understanding of the assembly of fibrils, and in particular, of their prefibrillar intermediates, must be achieved. This will facilitate proper targeting and design of fibrillogenesis inhibitors.

Acknowledgments—We thank Dr. Yuhui Xu for assistance with preparation of shadow casts, Dr. Tomas Ding for atomic force microscopy analysis, and Sara Vasquez for help in the preparation and maintenance of primary cultures. We acknowledge Drs. Dan Kirschner, David Howlett, Peter Lansbury, and John Maggio for critical comments and helpful discussions.

REFERENCES

1. Alzheimer, A. (1906) *Neurol. Centr.* **23,** 1129–1136
2. Teplow, D. B. (1998) *Amyloid: Int. J. Exp. Clin. Invest.* **5,** 121–142
3. Chartier-Harlin, M.-C., Crawford, F., and Houlden, H. (1991) *Nature* **353,** 844–846
4. Goate, A., Chartier-Harlin, M.-C., Mullan, M., Brown, J., Crawford, F., Fidani, L., Giuffra, L., Haynes, A., Irving, N., James, L., Mant, R., Newton, P., Rooke, K., Roques, P., Talbot, C., Pericak-Vance, M., Roses, A., Williamson, R., Rossor, M., Owen, M., and Hardy, J. (1991) *Nature* **349,** 704–706
5. Mullan, M., Crawford, F., Houlden, H., Axelman, K., Lilius, L., Winblad, B., and Lannfelt, L. (1992) *Nat. Genet.* **1,** 345–347
6. Eckman, C. B., Mehta, N. D., Crook, R., Perez-Tur, J., Prihar, G., Pfeiffer, E., Graff-Radford, N., Hinder, P., Yager, D., Zenk, B., Refolo, L. M., Prada, C. M., Younkin, S. G., Hutton, M., and Hardy, J. (1997) *Human Mol. Genet.* **6,** 2087–2089
7. Levy-Lahad, E., Wijsman, E. M., Nemens, E., Anderson, L., Goddard, K. A. B., Weber, J. L., Bird, T. D., and Schellenberg, G. D. (1995) *Science* **269,** 970–973
8. Levy-Lahad, E., Wasco, W., Poorkaj, P., Romano, D. M., Oshima, J., Pettingell, W. H., Yu, C. E., Jondro, P. D., Schmidt, S. D., Wang, K., Crowley, A. C., Fu, Y. H., Guenette, S. Y., Galas, D., Nemens, E., Wijsman, E. M., Bird, T. D., Schellenberg, G. D., and Tanzi, R. E. (1995) *Science* **269,** 973–977
9. Sherrington, R., Rogaev, E. I., Liang, Y., Rogaeva, E. A., Levesque, G., Ikeda, M., Chi, H., Lin, C., Li, G., Holman, K., Tsuda, T., Mar, L., Foncin, J. F., Bruni, A. C., Montesi, M. P., Sorbi, S., Rainero, I., Pinessi, L., Nee, L., Chumakov, I., Pollen, D., Brookes, A., Sanseau, P., Polinsky, R. J., Wasco, W., Da Silva, H. A. R., Haines, J. L., Pericak-Vance, M. A., Tanzi, R. E., Roses, A. D., Fraser, P. E., Rommen, J. M., and St. George-Hyslop, P. H. (1995) *Nature* **375,** 754–760
10. Selkoe, D. J. (1997) *Science* **275,** 630–631
11. Hardy, J. (1997) *Trends Neurosci.* **20,** 154–159
12. Corder, E. H., Saunders, A. M., Strittmatter, W. J., Schmechel, D. E., Gaskell, P. C., Small, G. W., Roses, A. D., Haines, J. L., and Pericak-Vance, M. A. (1993) *Science* **261,** 921–923
13. Blacker, D., Wilcox, M. A., Laird, N. M., Rodes, L., Horvath, S. M., Go, R. C., Perry, R., Watson, B., Jr., Bassett, S. S., McInnis, M. G., Albert, M. S., Hyman, B. T., and Tanzi, R. E. (1998) *Nat. Genet.* **19,** 357–360
14. Mattson, M. P. (1997) *Physiol. Rev.* **77,** 1081–1132
15. Geula, C., Wu, C. K., Saroff, D., Lorenzo, A., Yuan, M. L., and Yankner, B. A. (1998) *Nature Med.* **4,** 827–831
16. McKee, A. C., Kowall, N. W., Schumacher, J. S., and Beal, M. F. (1998) *Amyloid: Int. J. Exp. Clin. Invest.* **5,** 1–9
17. Soto, C., Sigurdsson, E. M., Morelli, L., Kumar, R. A., Castano, E. M., and Frangione, B. (1998) *Nature Med.* **4,** 822–826
18. Schenk, D. B., Rydel, R. E., May, P., Little, S., Panetta, J., Lieberburg, I., and Sinha, S. (1995) *J. Med. Chem.* **38,** 4141–4154
19. Ghanta, J., Shen, C. L., Kiessling, L. L., and Murphy, R. M. (1996) *J. Biol. Chem.* **271,** 29525–29528
20. Tjernberg, L. O., Naslund, J., Lindqvist, F., Johansson, J., Karlstrom, A. R., Thyberg, J., Terenius, L., and Nordstedt, C. (1996) *J. Biol. Chem.* **271,** 8545–8548
21. Jarrett, J. T., Berger, E. P., and Lansbury, P. T., Jr. (1993) *Biochemistry* **32,** 4693–4697
22. Harper, J. D., Wong, S. S., Lieber, C. M., and Lansbury, P. T. (1997) *Chem. Biol.* **4,** 119–125
23. Howlett, D. R., Jennings, K. H., Lee, D. C., Clark, M. S., Brown, F., Wetzel, R., Wood, S. J., Camilleri, P., and Roberts, G. W. (1995) *Neurodegeneration* **4,** 23–32
24. Wood, S. J., Maleeff, B., Hart, T., and Wetzel, R. (1996) *J. Mol. Biol.* **256,** 870–877
25. Snyder, S. W., Ladror, U. S., Wade, W. S., Wang, G. T., Barrett, L. W., Matayoshi, E. D., Huffaker, H. J., Krafft, G. A., and Holzman, T. F. (1994) *Biophys. J.* **67,** 1216–1228
26. Walsh, D. M., Lomakin, A., Benedek, G. B., Condron, M. M., and Teplow, D. B. (1997) *J. Biol. Chem.* **272,** 22364–22372
27. Harper, J. D., Lieber, C. M., and Lansbury, P. T. (1997) *Chem. Biol.* **4,** 951–959
28. Kuo, Y. M., Emmerling, M. R., Vigo-Pelfrey, C., Kasunic, T. C., Kirkpatrick, J. B., Murdoch, G. H., Ball, M. J., and Roher, A. E. (1996) *J. Biol. Chem.* **271,** 4077–4081
29. Lomakin, A., Chung, D. S., Benedek, G. B., Kirschner, D. A., and Teplow, D. B. (1996) *Proc. Natl. Acad. Sci. U. S. A.* **93,** 1125–1129
30. San Antonio, J. D., Lander, A. D., Karnovsky, M. J., and Slayter, H. S. (1994) *J. Cell Biol.* **125,** 1179–1188
31. Lomakin, A., Benedek, G. B., and Teplow, D. B. (1999) *Methods Enzymol.* **309,** in press
32. Klunk, W. E., Pettegrew, J. W., and Abraham, D. J. (1989) *J. Histochem. Cytochem.* **37,** 1273–1281
33. Naiki, H., and Nakakuki, K. (1996) *Lab. Invest.* **74,** 374–383
34. Perczel, A., Park, K., and Fasman, G. D. (1992) *Anal. Biochem.* **203,** 83–93
35. Brahms, S., and Brahms, J. (1980) *J. Mol. Biol.* **138,** 149–178
36. Hartley, D. M., Kurth, M. C., Bjerkness, L., Weiss, J. H., and Choi, D. W. (1993) *J. Neurosci.* **13,** 1993–2000
37. Hansen, M. B., Nielsen, S. E., and Berg, K. (1989) *J. Immunol. Methods* **119,** 203–210
38. Glenner, G. G. (1980) *New Engl. J. Med.* **302,** 1333–1343
39. Glenner, G. G. (1980) *New Engl. J. Med.* **302,** 1283–1292
40. Iversen, L. L., Mortishire-Smith, R. J., Pollack, S. J., and Shearman, M. S. (1995) *Biochem. J.* **311,** 1–16
41. Shearman, M. S., Ragan, C. I., and Iversen, L. L. (1994) *Proc. Natl. Acad. Sci. U. S. A.* **91,** 1470–1474
42. Shearman, M. S., Hawtin, S. R., and Tailor, V. J. (1995) *J. Neurochem.* **65,** 218–227
43. Liu, Y., and Schubert, D. (1997) *J. Neurochem.* **69,** 2285–2293
44. Kelly, J. W. (1998) *Curr. Opin. Struct. Biol.* **8,** 101–106
45. Roher, A., Wolfe, D., Palutke, M., and KuKuruga, D. (1986) *Proc. Natl. Acad. Sci. U. S. A.* **83,** 2662–2666
46. Selkoe, D. J., Abraham, C. R., Podlisny, M. B., and Duffy, L. K. (1986) *J. Neurochem.* **146,** 1820–1834
47. DeLellis, R. A., Glenner, G. G., and Ram, J. S. (1968) *J. Histochem. Cytochem.* **16,** 663–665
48. Klunk, W. E., Jacob, R. F., and Mason, R. P. (1999) *Anal. Biochem.* **266,** 66–76
49. Soto, C., Castaño, E. M., Frangione, B., and Inestrosa, N. C. (1995) *J. Biol. Chem.* **270,** 3063–3067
50. Soto, C., and Castaño, E. M. (1996) *Biochem. J.* **314,** 701–707
51. Clements, A., Allsop, D., Walsh, D. M., and Williams, C. H. (1996) *J. Neurochem.* **66,** 740–747
52. Barrow, C. J., Yasuda, A., Kenny, P. T. M., and Zagorski, M. (1992) *J. Mol. Biol.* **225,** 1075–1093
53. Pan, K. M., Baldwin, M., Nguyen, J., Gasset, M., Serban, A., Groth, D., Mehlhorn, I., Huang, Z., Fletterick, R. J., Cohen, F. E., and Prusiner, S. B. (1993) *Proc. Natl. Acad. Sci. U. S. A.* **90,** 10962–10966
54. Baldwin, M. A., Pan, K. M., Nguyen, J., Huang, Z., Groth, D., Serban, A., Gasset, M., Mehlhorn, I., Fletterick, R. J., Cohen, F. E., and Prusiner, S. B. (1994) *Phil. Trans. R. Soc. Lond. B Biol. Sci.* **343,** 435–441
55. Fezoui, Y., Weaver, D. L., and Osterhout, J. J. (1994) *Proc. Natl. Acad. Sci. U. S. A.* **91,** 3675–3679
56. Fezoui, Y., Connolly, P. J., and Osterhout, J. J. (1997) *Protein Sci.* **6,** 1869–1877
57. Seilheimer, B., Bohrmann, B., Bondolfi, L., Muller, F., Stuber, D., and Döbeli, H. (1997) *J. Struct. Biol.* **119,** 59–71
58. Lambert, M. P., Barlow, A. K., Chromy, B. A., Edwards, C., Freed, R., Liosatos, M., Morgan, T. E., Rozovsky, I., Trommer, B., Viola, K. L., Wals, P., Zhang, C., Finch, C. E., Krafft, G. A., and Klein, W. L. (1998) *Proc. Natl. Acad. Sci. U. S. A.* **95,** 6448–6453
59. Nybo, M., Svehag, S. E., and Nielsen, E. H. (1999) *Scand. J. Immunol.* **49,** 219–223
60. Inouye, H., Fraser, P. E., and Kirschner, D. A. (1993) *Biophys. J.* **64,** 502–519
61. Tomski, S. J., and Murphy, R. M. (1992) *Arch. Biochem. Biophys.* **294,** 630–638
62. Liu, Y. B., Peterson, D. A., and Schubert, D. (1998) *Proc. Natl. Acad. Sci. U. S. A.* **95,** 13266–13271
63. Abe, K., and Saito, H. (1998) *Neurosci. Res.* **31,** 295–305
64. Hartley, D. M., Walsh, D. M., Diehl, T. S., Teplow, D. B., and Selkoe, D. J. (1998) *Soc. Neurosci.* **24,** 508 (Abstr. 203.3)
65. Yankner, B. A., Duffy, L. K., and Kirschner, D. A. (1990) *Science* **250,** 279–282
66. Pike, C. J., Walencewicz, A. J., Glabe, C. G., and Cotman, C. W. (1991) *Brain Res.* **563,** 311–314
67. Pike, C. J., Burdick, D., Walencewicz, A. J., Glabe, C. G., and Cotman, C. W. (1993) *J. Neurosci.* **13,** 1676–1687
68. May, P. C., Gitter, B. D., Waters, D. C., Simmons, L. K., Becker, G. W., Small, J. S., and Robison, P. M. (1992) *Neurobiol. Aging* **13,** 605–607